Large-Scale Synthesis of TiO_2 Nanorods via Nonhydrolytic Sol−Gel Ester Elimination Reaction and Their Application to Photocatalytic Inactivation of *E. coli*

Jin Joo,[†,‡] Soon Gu Kwon,[†,‡] Taekyung Yu,[†,‡] Min Cho,[‡] Jinwoo Lee,[†,‡] Jeyong Yoon,[‡] and Taeghwan Hyeon*[,†,‡]

National Creative Research Initiative Center for Oxide Nanocrystalline Materials and School of Chemical and Biological Engineering, Seoul National University, Seoul 151-744, Korea

Received: May 11, 2005; In Final Form: June 20, 2005

A simple method of synthesizing a large quantity of TiO_2 nanorods was developed. A nonhydrolytic sol−gel reaction between titanium(IV) isopropoxide and oleic acid at 270 °C generated 3.4 nm (diameter) × 38 nm (length) sized TiO_2 nanocrystals. The transmission electron microscopic image showed that the particles have a uniform diameter distribution. X-ray diffraction and selected-area electron diffraction patterns combined with high-resolution transmission electron microscopic image showed that the TiO_2 nanorods are highly crystalline anatase crystal structure grown along the [001] direction. The diameters of the TiO_2 nanorods were controlled by adding 1-hexadecylamine to the reaction mixture as a cosurfactant. TiO_2 nanorods with average sizes of 2.7 nm × 28 nm, 2.2 nm × 32 nm, and 2.0 nm × 39 nm were obtained using 1, 5, and 10 mmol of 1-hexadecylamine, respectively. The optical absorption spectrum of the TiO_2 nanorods exhibited that the band gap of the nanorods was 3.33 eV at room temperature, which is 130 meV larger than that of bulk anatase (3.2 eV), demonstrating the quantum confinement effect. Oleic acid coordinated on the nanorod surface was removed by the reduction of the carboxyl group of oleic acid, and the Brunauer−Emmett−Teller surface area of the resulting naked TiO_2 nanorods was 198 m^2/g. The naked TiO_2 nanorods exhibited higher photocatalytic activity than the P-25 photocatalyst for the photocatalytic inactivation of *E. coli*.

Introduction

Titania (TiO_2) is an n-type wide band-gap semiconductor material and has been used in a wide variety of applications such as dye-sensitized solar cells (DSSCs),[1] photocatalysts,[2] photochromic devices,[3] and lithium batteries.[4] TiO_2 nanocrystals have been synthesized using various methods, including reactions in reverse micelles,[5] polyol reactions,[6] sonochemical synthesis,[7] and sol−gel reactions.[8] In most of these previous syntheses, the control of the reactivity of the titanium precursors, such as $TiCl_4$ and titanium alkoxides, was critical to synthesize high-quality TiO_2 nanocrystals, due to the high reactivity of the precursors. Moritz et al. reported the synthesis of uniform TiO_2 nanocrystals having various shapes from the reflux of the reaction mixtures with various ratios of Me_4NOH to titanium alkoxide.[8a,8b] However, the concentration of titanium alkoxide was so low that only a very small quantity of TiO_2 nanocrystals was produced. Weller et al. reported the controlled growth of TiO_2 by the modulation of the hydrolysis rate in the presence of oleic acid as a surfactant at 80 °C.[9] Adachi et al. synthesized anatase nanowires via a reactivity controlled hydrolysis of titanium(IV) isopropoxide and successfully applied to the electrodes for DSSCs.[10] Steigerwald et al. synthesized spherical TiO_2 nanocrystals from the reaction of organometallic bis-(cyclooctatetraene)titanium and dimethyl sulfoxide.[11]

Recently, nonhydrolytic sol−gel reactions have been successfully applied to the synthesis of nanocrystals of transition-metal oxides.[12] Colvin and co-workers synthesized TiO_2 nanocrystals via a nonhydrolytic alkyl halide elimination reaction (eq 1).[13] Our research group employed a similar procedure to produce ZrO_2 nanocrystals,[14] and Brus and co-workers further extended these synthetic methods to produce nanocrystals of HfO_2 and $Hf_XZr_{1-X}O_2$.[15] Recently, Cheon and co-workers reported the shape control of TiO_2 nanorods using the alkyl halide elimination reaction through the surfactant-assisted elimination of a high-energy facet.[16a] The Cheon group also synthesized nanorods of transition-metal oxides including those of TiO_2 from the thermal reaction of metal halides and oleic acid via acyl halide elimination process.[16b]

$$TiCl_4 + Ti(OPr^i)_4 \rightarrow TiO_2 + Cl{-}Pr^i \qquad (1)$$

However, this alkyl halide elimination route has certain intrinsic drawbacks in the synthesis of high-quality nanocrystals, which originate from the strong acidity of the Ti^{4+} cation in titanium-(IV) halide precursors. These highly acidic Ti(IV) species can react with the coordinating ligands via Lewis acid−base reactions because the ligands generally used in the synthesis of nanocrystals are Lewis bases. For example, the fatty amine forms a salt with $TiCl_4$, and the fatty acid reacts with $TiCl_4$ to produce titanium(IV) carboxylate and HCl. These reactions compete with the nonhydrolytic sol−gel reaction, which constitutes a significant obstacle to the size and shape control of the TiO_2 nanocrystals and a large-scale production.

One-dimensional (1-D) nanostructured materials including nanorods and nanowires have received a tremendous amount of attention because of their unique properties derived from low dimensionality and quantum confinement effect and their many potential applications including interconnects and functional

* To whom correspondence should be addressed. E-mail: thyeon@plaza.snu.ac.kr.

[†] National Creative Research Initiative Center for Oxide Nanocrystalline Materials.

[‡] School of Chemical and Biological Engineering.

10.1021/jp052458z CCC: $30.25
Published on Web 07/27/2005

blocks for fabricating nanoscale devices.[17] Many 1-D nanocrystals of magnetic materials,[18] II−IV semiconductors,[19] and metals[20] have been synthesized using various procedures. Herein we report on the synthesis of TiO_2 nanorods from a nonhydrolytic ester elimination reaction of titanium(IV) alkoxide and oleic acid. Furthermore, we removed the stabilizing surfactants from the TiO_2 nanorods without aggregation and successfully used the naked nanorods for photocatalytic inactivation of *E. coli*.

Experimental Section

Chemicals. All experimental procedures were conducted in an argon atmosphere using standard Schlenk techniques. 1-Hexadexylamine (HDA, Aldrich, 98%), decanoic acid (Aldrich, 99%), and oleic acid (OA, TCI, 99%) were degassed at 110 °C for 1 h under a vacuum to remove trace water and oxygen. Titanium(IV) isopropoxide (TTIP, Aldrich, 99.99%) and titanium(IV) butoxide (Aldrich, 97%) were used as received.

Synthesis of TiO_2 Nanorods. TTIP (17.7 mL, 60 mmol) was added to 50 g of OA at room temperature. Then, the resulting mixture was gradually heated to 270 °C for a period of 20 min and kept at this temperature for 2 h. The resulting light-yellow clear solution gradually turned white. The solution was then cooled to room temperature, and excess ethanol was added to yield a white precipitate, which was then separated by centrifuging. The resulting white powder could easily be re-dispersed in nonpolar organic solvents, such as hexane and chloroform. The prepared TiO_2 nanocrystals were composed of nanorods and 3.0 nm sized spherical nanocrystals. About 3.5 g of nanocrystals was obtained from this synthesis (yield of ~70%). Pure TiO_2 nanorods were obtained by conducting size-selective precipitation from a hexane/ethanol solution containing the product mixture. The diameter of the nanorods was controlled by adding different amounts of 1-hexadexylamine (10, 5, and 1 mmol) in the reaction mixture while keeping the other synthetic conditions unchanged. We were able to synthesize as much as 11.6 g of TiO_2 nanocrystals when 35 mL of TTIP (120 mmol) and 100 g of OA was reacted (see Supporting Information for transmission electron microscopy (TEM) image and photograph).

Removal of Surfactant from the TiO_2 Nanorods. Oleic acid (OA) coordinated on the TiO_2 nanorods was removed by reducing the carboxylic group in OA. First, dried TiO_2 nanorods were placed in a 100-mL round-bottomed flask under an argon atmosphere. Superhydride solution (10 mL, 1 M lithium triethylborohydride in THF) was added dropwise with vigorous stirring at room temperature, resulting in the release of hydrogen gas due to the reduction of the OA on the surface of the TiO_2 nanocrystals. After the complete addition of the superhydride solution, the resulting solution was sonicated for 30 min, following which a white precipitate was obtained by centrifugation. These superhydride reduction processes were repeated three times for the complete reduction of OA. Then, fresh THF was added to wash the residual superhydride, and the precipitate retrieved by centrifugation. This THF washing procedure was repeated several times for the complete washing. The resulting naked TiO_2 nanocrystal powder is dispersable in water.

Characterization of Nanocrystals. The synthesized nanocrystals were characterized by low- and high-resolution (HR) TEM and powder X-ray diffraction (XRD). The TEM images were obtained on a JEOL EM-2010 microscope. The X-ray diffraction patterns were obtained with a Rigaku D/Max-3C diffractometer, equipped with a rotating anode and a Cu Kα radiation source ($\lambda = 0.15418$ nm). Gas chromatographs were obtained on a Hewlett-Packard HP5890 series II gas chromatograph. The optical absorption was characterized at room temperature with a Shimadzu UV-3100 spectrometer. A thin film of TiO_2 nanorods was prepared using a spin coater. Infrared (IR) spectra were collected on a Mettler Toledo ReactIR 4000 and a Bomem DA 8 spectrometer. The surface area was determined from the Brunauer−Emmett−Teller (BET) equation, using a Micromeritics ASAP 2000 at 77 K.

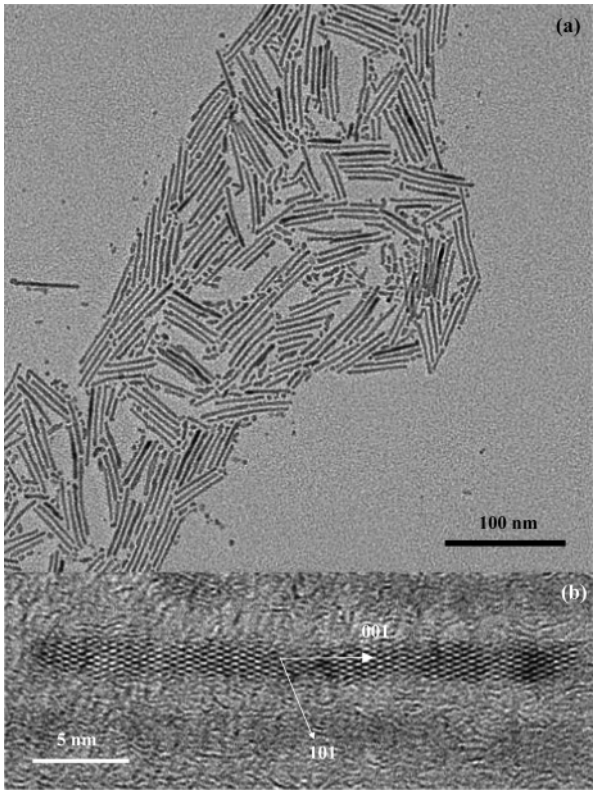

Figure 1. (a) TEM image of as-synthesized TiO_2 nanocrystals. (b) HRTEM image of TiO_2 nanorods.

Photocatalytic Inactivation of *E. coli*. In photocatalytic inactivation experiments, TiO_2 nanocrystals and P-25 (Degussa Co.) were used. Photocatalytic experiments are conducted as described by Cho et al.,[21] using 60-mL Pyrex reactors (UV cutoff < 300 nm) with 50 mL of reaction solution and black light blue lamps (BLB lamp, 18 W, Philips Co.). Experiments were conducted at a constant temperature of 20 °C, at a controlled pH of 7.1 (phosphate buffer), and at a constant light intensity of 7.9×10^{-6} Einsteins/L/s, which was measured by ferrioxalate actinometry. The slurry of TiO_2 (1 g/L)/*E. coli* (3×10^5 cfu/mL) was intensively mixed with magnetic stirrer, and five samples were collected for 10−130 min to measure the population of *E. coli*. Viable concentration of *E. coli* was measured with spreading plate method. In the control test, no inactivation of *E. coli* was observed in the absence of either BLB radiation or TiO_2 particles within the present experimental time scale. Experiments were repeated three times to confirm their reproducibility, and their averaged values with statistical deviation were used for the data analysis.

Results and Discussion

The XRD pattern of the prepared TiO_2 nanocrystals was consistent with that of the anatase crystal structure (see Supporting Information). The greater intensity of the (004) peak compared to that of the (002) peak is indicative of the anisotropy of the TiO_2 nanocrystals. Figure 1a shows the TEM image of the as-synthesized TiO_2 nanocrystals, which consist of nanorods with an average size of 3.4 nm (diameter) × 38 nm (length)

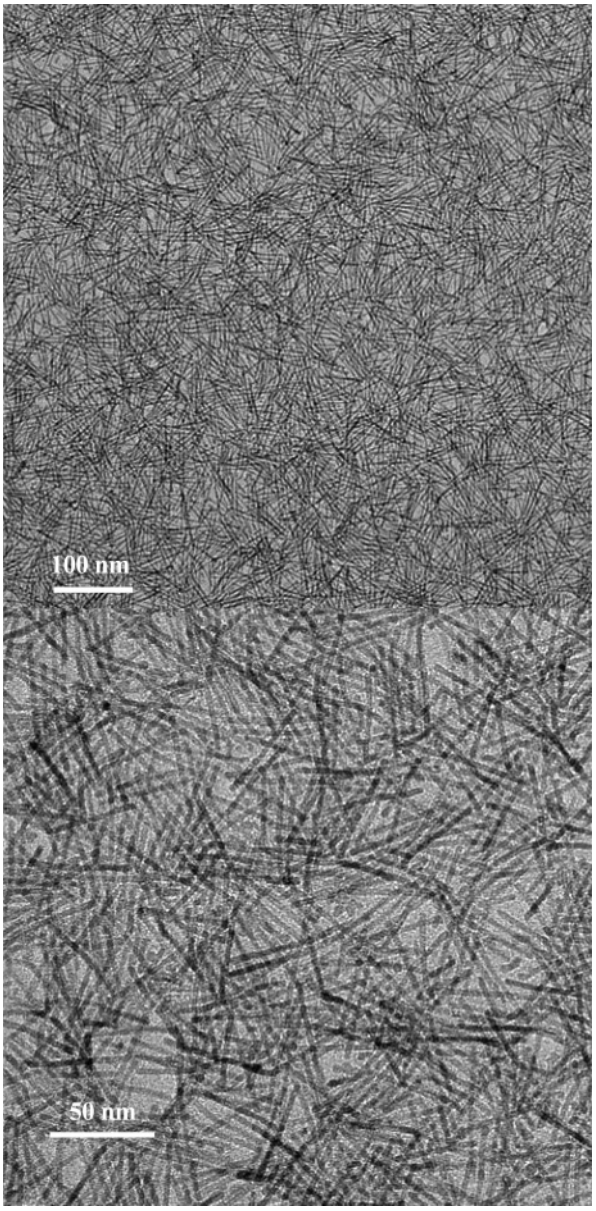

Figure 2. TEM images of TiO_2 nanorods after one cycle of size-selective precipitation.

and quasi-spherical nanocrystals with an average diameter of 3.0 nm. The relative population of the nanorods is over 70%. The HRTEM image of a single nanorod shown in Figure 1b and the selected-area electron diffraction (SAED) pattern, which has a [010] zone axis, show that the nanorods were highly crystalline and that they grew along the [001] direction, which is consistent with the greater intensity of the (004) diffraction peak of the TiO_2 nanorods compared to that of bulk anatase crystal (see Supporting Information). The fast growth along the [001] direction is typical of anatase phase,[8a,8b,9,22] and results from the 1.4 times higher surface energy of the {001} surfaces in comparison to that of the {101} surfaces, as predicted by the Donnay−Harker rules.[23] Banfield proposed another mechanism of rapid growth on {001} faces,[22] in which only the {001} surfaces can generate continual reactive sites for the crystal growth. Pure TiO_2 nanorods were obtained after one cycle of size-selective precipitation process, and the TEM image (Figure 2) shows that no quasispherical nanocrystal was observed.

We were able to control the diameters of the TiO_2 nanorods by adding different amounts of HDA into the reaction mixture composed of titanium(IV) isopropoxide and oleic acid. The amine group is known to form a strong bond with the Ti^{4+} cation on the rutile (110) surface.[24] By consideration of the similarity of the rutile (110) surface to that of anatase (101), it was anticipated that the growth of the (101) surface of the TiO_2 nanorods could be limited by varying the amount of HDA. The TEM images of the synthesized TiO_2 nanorods capped with HDA are shown in Figure 3. The average diameters of the nanorods were 2.7, 2.2, and 2.0 nm, and their lengths were 28, 32, and 39 nm when the amount of HDA was 1, 5, and 10 mmol, respectively (see Supporting Information for the diameter distributions).

Figure 4 shows the Fourier transform IR (FTIR) spectra of a complex of TTIP−OA and the TiO_2 nanocrystals. The TTIP−OA complexes were obtained by the reaction of TTIP with OA at 100 °C. In the spectrum for the TTIP−OA complexes in Figure 4a, the two absorption bands at 1008 and 1125 cm^{-1} result from the stretching vibrations of the O−C−C and C−C bonds, respectively, of the isopropyl groups of TTIP.[25,26] Two absorption bands are observed at 1457 and 1544 cm^{-1} in Figure 4a, which are attributed to the symmetric and asymmetric stretching vibrations of the carboxylate groups, respectively. The separation of these bands ($\Delta\upsilon$) indicates coordination modes of TTIP and the carboxylic group, viz., monodentate ($\Delta\upsilon$ = 425 cm^{-1}), bidentate chelating ($\Delta\upsilon$ = 130−80 cm^{-1}), and bidentate bridging ($\Delta\upsilon$ = 140−160 cm^{-1}). The two bands observed in the IR spectrum of a TTIP−OA complex are therefore attributed to the bidentate chelating of the oleate anions to TTIP ($\Delta\upsilon$ = 87 cm^{-1}).[27] The absorption band at 1600 cm−1 results from the bending vibration of the Ti−OH bonds,[27b,28] produced by the nonhydrolytic sol−gel reaction of TTIP and OA. The carbonyl band originating from the free ester at 1741 cm^{-1} and the bending vibration of Ti−OH at 1600 cm^{-1} clearly show that the nonhydrolytic sol−gel reaction of OA and TTIP produces the ester and Ti−OH. These hydroxide groups in Ti−OH form the TiO_2 nanocrystals by the condensation reaction at elevated temperature.

The produced ester was characterized by the gas chromatography mass spectroscopy (GC-MS) analysis. In the GC-MS experiment, titanium(IV) butoxide and decanoic acid were used because butyl decanoate has much lower boiling point than isopropyl oleate, which can be purified by simple vacuum distillation, and is easier to characterize. The GC-MS spectra clearly indicate that the nonhydrolytic sol−gel reaction of titanium(IV) butoxide and decanoic acid generates butyl decanoate, confirming ester elimination reaction (see Supporting Information). The FTIR spectrum of the TiO_2 nanocrystals is shown in Figure 4b. The observed symmetric (1425 cm^{-1}) and asymmetric (1525 cm^{-1}) stretching vibrations of the carboxylate groups are characteristic of the bidentate chelating mode. The two sharp absorption bands at 2855 and 2925 cm^{-1} are attributed to the symmetric and asymmetric CH_2 stretching vibrations of OA, respectively. The following equations describe a proposed mechanism based on the FTIR results and the byproduct analysis using GC-MS.

$$\equiv Ti{-}OPr^{i} + HOOC(CH_2)_7CH{=}CH(CH_2)_7CH_3 \rightarrow \equiv Ti{-}OH + Pr^{i}OC(=O)(CH_2)_7CH{=}CH(CH_2)_7CH_3 \quad (2)$$

$$\equiv Ti{-}OH + OH{-}Ti\equiv \rightarrow TiO_2 + H_2O \quad (3)$$

When OA was removed by reducing the carboxylate groups with superhydride, these bands disappeared, as shown in Figure 4c. This reveals that the OA coordinated to the TiO_2 nanorods was completely removed by the reduction at room temperature.

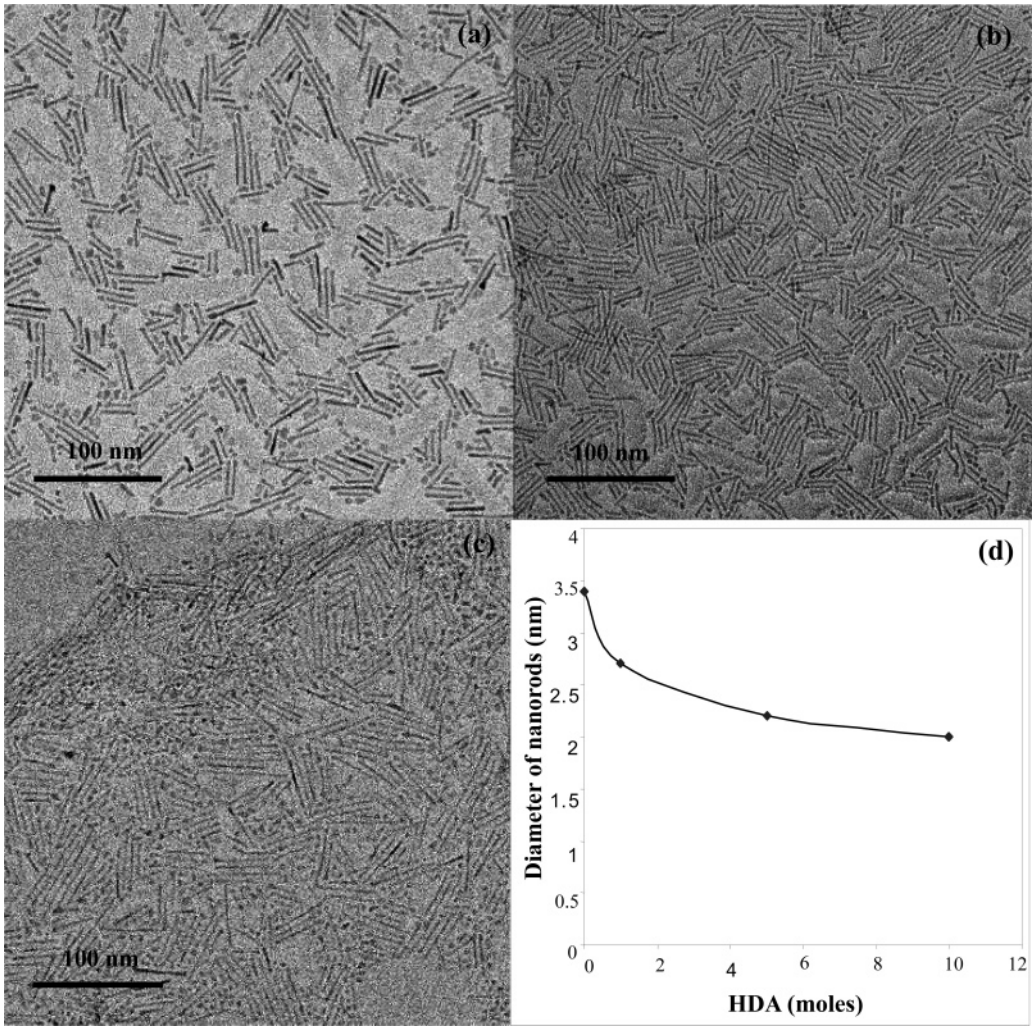

Figure 3. TEM images of diameter controlled TiO_2 nanorods with an average size of **(**a**)** 2.7 nm (diameter) × 28 nm (length), **(**b**)** 2.2 nm × 32 nm, and **(**c**)** 2.0 nm × 39 nm. **(**d**)** Diameter variation with an amount of HDA.

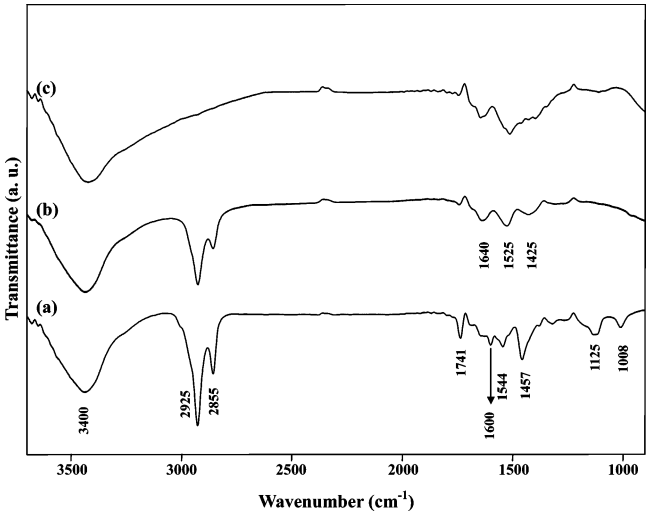

Figure 4. FTIR spectra of **(**a**)** complex of titanium(IV) isopropoxide and OA, **(**b**)** as-synthesized TiO_2 nanorods, and **(**c**)** TiO_2 nanorods after the superhydride reduction.

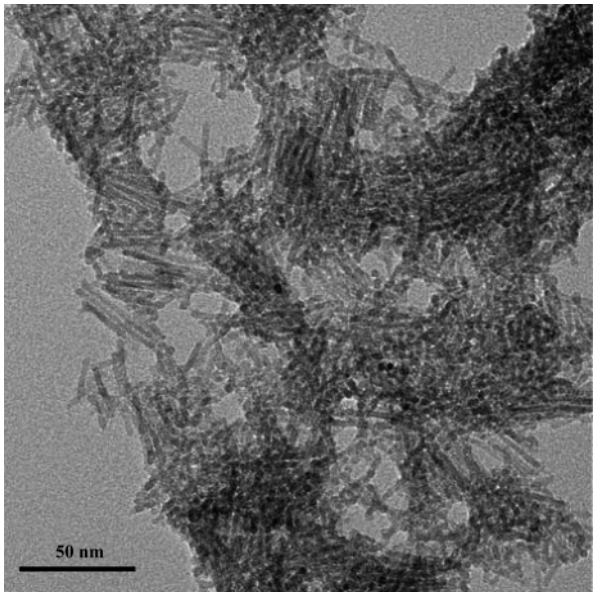

Figure 5. TEM images of TiO_2 nanorods after the removal of OA by the superhydride reduction.

The TEM image of the naked TiO_2 nanorods, shown in Figure 5, showed that the nanorods maintained their initial rod-shaped morphology and that they are not agglomerated. It is important to remove the stabilizing surfactant from the nanocrystals without agglomeration, because the surfactant molecules coordinated on the surface of the nanocrystals act as an obstacle in many applications. Especially, in the photocatalytic application of TiO_2 nanocrystals, the reactant cannot approach the surface of the nanocrystals due to the ligand coordinated to the surface of the nanocrystals. Thus, it would seem that this room-

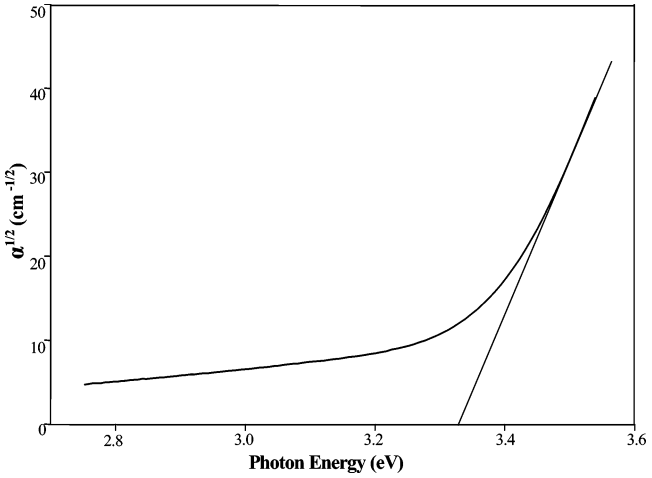

Figure 6. Optical absorption spectrum ($\alpha^{1/2}$ vs photon energy (E)) of TiO_2 nanorods.

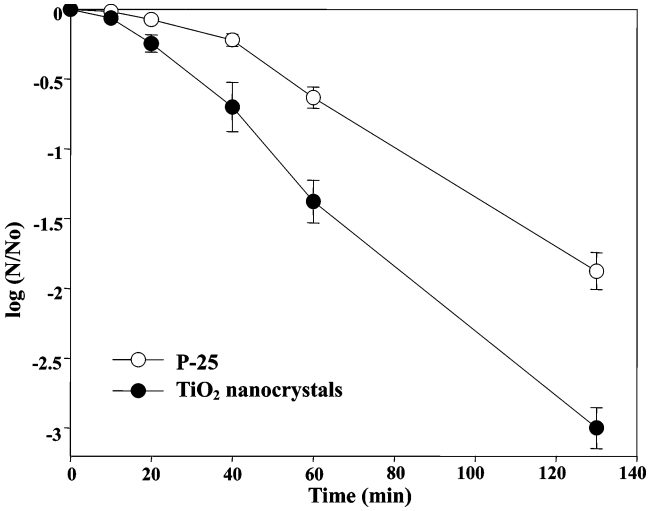

Figure 7. The photocatalytic inactivation of *E. coli* using naked TiO_2 nanocrystals and Degussa P-25 as photocatalysts.

temperature reduction process represents a promising method for obtaining naked nanocrystals without agglomeration. The BET surface area of the TiO_2 nanorods after the removal of OA was 198 m^2/g, and they are highly dispersable in water, which is very important for many applications in aqueous media. All of the spectra shown in Figure 4 show broad bands at 3400 cm^{-1} and between 1650 and 1630 cm^{-1}, which correspond to the water absorbed on the surface and the hydroxyl groups of the TiO_2 nanorods.[26,28,29] By consideration of the extremely hydrophobic nature of the TiO_2 nanorods, whose surface is capped with OA, it is interesting to note that there is a considerable number of hydroxyl groups on the surface of the TiO_2 nanorods, as shown in parts b and c of Figure 4. These water molecules absorbed on the surface and hydroxyl groups play an important role in photocatalytic applications, because these species produce hydroxyl radicals from their reaction with photogenerated holes on the TiO_2 surfaces, which act as a powerful oxidant in the inactivation of microorganisms.[21a]

The band gap of the TiO_2 nanorods were estimated using the approximate relation, $T = [(1 - R)^2\ e^{-\alpha d}]/[1 - R^2\ e^{-\alpha d}]$, where T is the transmittance and R is the reflectivity. The absorption coefficient (α) is dependent on $(E - E_g)^2$ above the threshold of fundamental absorption in the indirect allowed transition. $\alpha^{1/2}$ is plotted against the photon energy (E) in Figure 6. The extrapolation shows that the TiO_2 nanorods have an optical absorption gap of 3.33 eV at room temperature, which is 130 meV larger than that of bulk anatase (3.2 eV).[30] Brus reported that the radius (r) of an exciton can be expressed in terms of $r = a_o\epsilon/(m_e^*/m_e)$, where a_o is the Bohr radius and m_e^* is the effective mass.[31] On the basis of previous reports concerning the effective mass of TiO_2, the exciton radius of TiO_2 was calculated to be in the range of 7.5−1.9 nm (e.g., $\epsilon = 31$, $m_e^* = 1\ m_e$).[30,32] Thus, it can be explained that 130 meV shift in the band gap of the TiO_2 nanorods results from the quantum size effect, which is governed by the diameter of the TiO_2 nanorods (3.4 nm) rather than their length (38 nm). The diameter dependence of the band gap of the nanorods is a well-known phenomenon in the case of II−IV semiconductor nanocrystals.[33] In photocatalytic applications, it is well known that an increased band gap enhances the photocatalytic efficiency.[34] By consideration of the photocatalytic process as an electrochemical cell, a larger band gap increases the redox potential in eq 4, where E is the band gap of the semiconductor, ΔG is the free energy change of the redox process, Z is an integer corresponding to the number of elementary charges, and F is the Faraday constant.[35]

$$\Delta G = -ZEF \tag{4}$$

The photocatalytic activity of the TiO_2 nanorods was characterized by evaluating their ability to inactivate *E. coli*, as compared with that of a commercially available P-25 photocatalyst, which is known to be the most powerful oxidant in photocatalysis. Figure 7 shows that 99% of the *E. coli* was inactivated after 92 and ~140 min by the TiO_2 nanorods and P-25, respectively. Since the photochemical sterilization of *E. coli* using Pt−TiO_2 was first reported by Mutsunaga et al. in 1985,[36] many photocatalytic disinfection studies using TiO_2 have been carried out on the inactivation of micro-organisms,[21,37−41] which demonstrate that the hydroxyl radical, originating from the hydroxyl groups on the TiO_2 surface, is mainly responsible for the inactivation of the micro-organism. Thus, the strong photocatalytic activity of the TiO_2 nanorods can be attributed to three separate factors, viz., their high surface area of up to 198 m^2/g, the large amount of hydroxyl radicals on the surface of the nanorods, and their larger band gap, as compared with that of bulk anatase, which results from the quantum confinement effect of the TiO_2 nanorods.

Conclusions

TiO_2 nanorods with dimensions of 3.4 nm (diameter) × 38 nm (length) were synthesized using a nonhydrolytic ester elimination reaction between titanium(IV) isopropoxide and OA. The TiO_2 nanorods have a single crystalline anatase phase. Diameter control was achieved in the range of 2.0−3.4 nm by adding various amounts of HDA into the reaction mixture. The OA surfactant was removed by a simple reduction at room temperature. The resulting naked TiO_2 nanorods exhibited higher photocatalytic activity than a commercial P-25 photocatalyst for the photocatalytic inactivation of *E. coli*. This enhanced photocatalytic activity seems to result from their high surface area, large amount of surface hydroxyl group, and the increased band gap of the TiO_2 nanorods.

Acknowledgment. The work was supported by the National Creative Research Initiative Program of the Korean Ministry of Science and Technology.

Supporting Information Available: HRTEM image and SAED pattern of TiO_2 nanorods. Diameter distribution histograms of TiO_2 nanorods synthesized using various amounts of

HDA. GC-MS spectra of the byproduct of the reaction between Ti(IV) butoxide and decanoic acid. XRD patterns of TiO_2 nanorods before and after superhydride reduction of OA. Photograph and TEM image of TiO_2 nanocrystals synthesized in a large quantity of >11 g. This material is available free of charge via the Internet at http://pubs.acs.org.

References and Notes

(1) (a) O'Regan, B.; Grätzel, M. *Nature* **1991**, *353*, 737. (b) Hagfeldt, A.; Grätzel, M. *Chem. Rev.* **1995**, *95*, 49. (c) Yan, S. G.; Prieskorn, J. S.; Kim, Y. J.; Hupp, J. T. *J. Phys. Chem. B* **2000**, *104*, 10871. (d) Lemon, B. I.; Hupp, J. T. *J. Phys. Chem. B* **1999**, *103*, 3797. (e) Kamat, P. V. *Chem. Rev.* **1993**, *93*, 267.

(2) (a) Kamat, P. V. *J. Phys. Chem. B* **2002**, *106*, 7729. (b) Subramanian, V.; Wolf, E.; Kamat, P. V. *J. Phys. Chem. B* **2001**, *105*, 11439. (c) Cho, Y.; Choi, W.; Lee, C.-H.; Hyeon, T.; Lee, H.-I. *Environ. Sci. Technol.* **2001**, *35*, 2988.

(3) Iuchi, K.; Ohko, Y.; Tatsuma, T.; Fujishima, A. *Chem. Mater.* **2004**, *16*, 1165.

(4) Wagemaker, M.; Krol, R. V. D.; Kentgens, A. P. M.; Well, A. A. V.; Mulder, F. M. *J. Am. Chem. Soc.* **2001**, *123*, 11454.

(5) (a) Stathatos, E.; Lianos, P. *Langmuir* **1997**, *13*, 4295. (b) Wu, M.; Long, J.; Huang, A.; Luo, Y. *Langmuir* **1999**, *15*, 8822. (c) Lin, J.; Lin, Y.; Liu, P.; Meziani, M. J.; Allard, L. F.; Sun, Y. *J. Am. Chem. Soc.* **2002**, *124*, 11514.

(6) Feldmann, C.; Jungk, H. *Angew. Chem., Int. Ed.* **2001**, *40*, 359.

(7) Zhu, Y.; Li, H.; Koltypin, Y.; Hacohen, Y. R.; Gedanken, A. *Chem. Commun.* **2001**, 2616.

(8) (a) Moritz, T.; Reiss, J.; Diesner, K.; Su, D.; Chemseddine, A. *J. Phys. Chem. B* **1997**, *101*, 8052. (b) Chemseddine, A.; Moritz, T. *Eur. J. Inorg. Chem.* **1999**, 235. (c) Kasuga, T.; Hiramatsu, M.; Hoson, A.; Sekino, T.; Niihara, K. *Langmuir* **1998**, *14*, 3160. (d) Kasuga, T.; Hiramatsu, M.; Hoson, A.; Sekino, T.; Niihara, K. *Adv. Mater.* **1999**, *11*, 1307. (e) Chen, Q.; Zhou, W.; Du, G.; Peng, L. *Adv. Mater.* **2002**, *14*, 1208. (f) Bacsa, R. R.; Grätzel, M. *J. Am. Ceram. Soc.* **1996**, *79*, 2185. (g) Yanagisawa, K.; Ovenstone, J. *J. Phys. Chem. B* **1999**, *103*, 7781. (h) Aruna, S. T.; Tirosh, S.; Zaban, A. *J. Mater. Chem.* **2000**, *10*, 2388. (i) Yin, H.; Wada, Y.; Kitamura, T.; Kambe, S.; Murasawa, S.; Mori, H.; Sakata, T.; Yanagida, S. *J. Mater.* Chem. **2001**, *11*, 1694.

(9) Cozzoli, P. D.; Kornowski, A.; Weller, H. *J. Am. Chem. Soc.* **2003**, *125*, 14539.

(10) Adachi, M.; Murata, Y.; Takao, J.; Jiu, J.; Sakamoto, M.; Wang, F. *J. Am. Chem. Soc.* **2004**, *126*, 14943.

(11) Tang, J.; Redl, F.; Zhu, Y.; Siegrist, T.; Brus, L. E.; Steigerwald, M. L. *Nano Lett.* **2005**, *5*, 543.

(12) Vioux, A. *Chem. Mater.* **1997**, *9*, 2292.

(13) Trentler. T. J.; Denler, T. E.; Bertone, J. F.; Agrawal, A.; Colvin, V. L. *J. Am. Chem. Soc.* **1999**, *121*, 1613.

(14) Joo, J.; Yu, T.; Kim, Y. W.; Park, H. M.; Wu, F.; Zhang, J. Z.; Hyeon, T. *J. Am. Chem. Soc.* **2003**, *125*, 6553.

(15) Tang, J.; Fabbri, J.; Robinson, R. D.; Zhu, Y.; Herman, I. P.; Steigerwald, M. L.; Brus, L. E. *Chem. Mater.* **2004**, *16*, 1336.

(16) (a) Jun, Y.-w.; Casula, M. F.; Sim, J.-H.; Kim, S. Y.; Cheon, J.; Alivisatos, A. P. *J. Am. Chem. Soc.* **2003**, *125*, 15981. (b) Seo, J.-w.; Jun, Y.-w.; Ko, S. J.; Cheon, J. *J. Phys. Chem. B* **2005,** *109*, 5389.

(17) (a) Xia, Y.; Yang, P.; Sun, Y.; Wu, Y.; Mayers, B.; Gates, B.; Yin, Y.; Kim, F.; Yan, H. *Adv. Mater.* **2003**, *15*, 353. (b) Hu, J.-T.; Odom, T. W.; Lieber, C. M. *Acc. Chem. Res.* **1999**, *32*, 435. (c) Lee, S.-M.; Cho, S.-N.; Cheon, J. *Adv. Mater.* **2003,** *15*, 441.

(18) (a) Park, S.-J.; Kim, S.; Lee, S.; Khim, Z. G.; Char, K.; Hyeon, T. *J. Am. Chem. Soc.* **2000**, *122*, 8581. (b) Park, J.; Koo, B.; Hwang, Y.; Bae, C.; An, K.; Park, J.-G.; Park, H. M.; Hyeon, T. *Angew. Chem., Int. Ed.* **2004**, *43*, 2282. (c) Dumestre, F.; Chaudret, B.; Amiens, C.; Fromen, M. C.; Casanove, J.; Renaud, P.; Zurcher, P. *Angew. Chem., Int. Ed.* **2002**, *41*, 4286. (d) Dumestre, F.; Chaudret, B.; Amiens, C.; Respaud, M.; Fejes, P.; Renaud, P.; Zurcher, P. *Angew. Chem., Int. Ed.* **2003**, *42*, 5213.

(19) (a) Joo, J.; Na, H. B.; Yu, T.; Yu, J. H.; Kim, Y. W.; Wu, F.; Zhang, J. Z.; Hyeon, T. *J. Am. Chem. Soc.* **2003**, *125*, 11100. (b) Yu, J. H.; Joo, J.; Park, H. M.; Baek, S.-I.; Kim, Y. W.; Hyeon, T. *J. Am. Chem. Soc.* **2005**, *127*, 5662. (c) Peng, X.; Manna, L.; Yang, W.; Wickham, J.; Scher, E.; Kadavanich, A.; Alivisatos, A. P. *Nature* **2000**, *404*, 59. (d) Peng, Z. A.; Peng, X. G. *J. Am. Chem. Soc.* **2001**, *123*, 183. (e) Huynh, W. U.; Dittmer, J. J.; Alivisatos, A. P. *Science* **2002**, *295*, 2425. (f) Jun, Y.-w.; Lee, S.-M.; Kang, N.-J.; Cheon, J. *J. Am. Chem. Soc.* **2001**, *123*, 5150. (g) Holmes, D.; Doty, R. C.; Johnston, K. P.; Korgel, B. A. *Science* **2000**, *287*, 1471. (h) Hanrath, T.; Korgel, B. A. *J. Am. Chem. Soc.* **2002**, *124*, 1424. (i) Tang, Z.; Kotov, N. A.; Giersig, M. *Science* **2002**, *297*, 237. (j) Yu, H.; Li, J.; Loomis, R. A.; Gibbons, P. C.; Wang, L. W.; Buhro, W. E. *J. Am. Chem. Soc.* **2003**, *125*, 16168. (k) Kan, S.; Mokari, T.; Rothenberg, E.; Banin, U. *Nat. Mater.* **2003**, *2*, 155. (l) Yu, H.; Li, J.; Loomis, R. A.; Wang, L.-W.; Buhro, W. E. *Nat. Mater.* **2003**, *2*, 517.

(20) (a) Murphy, C. J.; Jana, N. R. *Adv. Mater.* **2002**, *14*, 80. (b) Jana, N. R.; Gearheart, L.; Murphy, C. J. *J. Phys. Chem. B* **2001**, *105*, 4065. (c) Busbee, B. D.; Obare, S. O.; Murphy, C. J. *Adv. Mater.* **2003**, *15*, 414. (d) Xiong, Y.; Xie, Y.; Wu, C.; Yang, J.; Li, Z.; Xu, F. *Adv. Mater.* **2003**, *15*, 405.

(21) (a) Cho, M.; Chung, H.; Choi, W.; Yoon, J. *Water Res.* **2004**, *38*, 1069. (b) Cho, M.; Chung, H.; Choi, W.; Yoon J. *Appl. Environ. Microbiol.* **2005**, *71*, 270.

(22) (a) Penn, R. L.; Banfield, J. F. *Geochim. Cosmichim. Acta* **1999**, *63*, 1549. (b) Zhang, H. Z.; Banfield, J. F. *Chem. Mater.* **2002**, *14*, 4145. (c) Zhang, H. Z.; Finnegan, M.; Banfield, J. F. *Nano Lett.* **2001**, *1*, 81. (d) Zhang, H. Z.; Banfield, J. F. *J. Phys. Chem. B* **2000**, *104*, 3481.

(23) Donnay, J. D.; Harker, D. *Am. Miner.* **1937**, *22*, 446.

(24) Farfan-Arribas, E.; Madix, R. J. *J. Phys. Chem. B* **2003**, *107*, 3225.

(25) Gun'ko, V. M.; Zarko, V. I.; Turov, V. V.; Leboda, R.; Chibowski, E.; Holysz, L.; Pakhlov, E. M.; Voronin, E. F.; Dudnik, V. V.; Gornikov, Y. I. *J. Colloid Interface Sci.* **1998**, *198*, 141.

(26) Nakayama, T. *J. Electrochem. Soc.* **1994**, *141*, 237.

(27) (a) Murakami, Y.; Matsumoto, T.; Takasu, Y. *J. Phys. Chem. B* **1999**, *103*, 1836. (b) Hwang, U.-Y.; Park, H.-S.; Koo, K.-K. *Ind. Eng. Chem. Res.* **2004**, *43*, 728.

(28) Sanchez, E.; Lopez, T.; Gomea, R.; Morales, A.; Novaro, O. *J. Solid State Chem.* **1996**, *122*, 309.

(29) (a) Ding, Z.; Lu, G. Q.; Greenfield, P. F. *J. Phys. Chem. B* **2000**, *104*, 4815. (b) Suda, Y.; Morimoto, T. *Langmuir* **1987**, *3*, 786. (c) Tanaka, K.; White, J. M. *J. Phys. Chem.* **1982**, *86*, 4708.

(30) (a) Tang, H.; Prasad, K.; Sanjinès, R.; Schmid, P. E.; Lèvy, F. *J. Appl. Phys.* **1994**, *75*, 2042. (b) Kormann, C.; Bahnemann, D. W.; Hoffmann, M. R. *J. Phys. Chem.* **1988**, *92*, 5196.

(31) Brus, L. E. *J. Phys. Chem.* **1986**, *90*, 2555.

(32) (a) Acket, G. A.; Volger, J. *Physica* **1966**, *32*, 1680. (b) Pascual, J.; Camassel, J.; Mathieu, H. *Phys. Rev. B: Condens. Matter* **1978**, *18*, 5606. (c) Agekyan, V. T.; Berezhnaya, A. A.; Lutsenko, V. V.; Stepanov, Y. A. *Sov. Phys. Solid State* **1980**, *22*, 6.

(33) (a) Yin, M.; Gu, Y.; Kuskovsky, I. L.; Andelman, T.; Zhu, Y.; Neumark, G. F.; O'Brien, S. *J. Am. Chem.* Soc. **2004**, *126*, 6206. (b) Li, L.-s.; Hu, J.; Yang, W.; Alivisatos, A. P. *Nano Lett.* **2001**, *1*, 349.

(34) (a) Yu, J. C.; Zhang, L.; Yu, J. *Chem. Mater.* **2002**, *14*, 4647. (b) Lin, J.; Yu, J. C.; Lo, D.; Lam, S. K. *J. Catal.* **1999**, *183*, 368.

(35) Hibbert, D. B. *Introduction to Electrochemistry*; Macmillan: London, 1993.

(36) Mutsunaga, T.; Tomodam, R.; Nakajima, T.; Wake, H. *FEMS Microbiol. Lett.* **1985**, *29*, 211.

(37) Kikuchi, Y.; Sunada, K.; Iyoda, T.; Hashimoto, K.; Fujishima, A. *J. Photochem. Photobiol., A* **1997**, *160*, 51.

(38) Lee, S.; Otaki, N. M.; Ohgaki, S. *Water Sci. Technol.* **1997**, *35*, 101.

(39) Watts, R. J.; Kong, S.; Orr, M. P.; Miller, G. C.; Henry, B. E. *Water Res.* **1995**, *29*, 95.

(40) Wei, C.; Lin, W.; Zainal, Z.; Zhu, N. E.; Kruzic, K.; Smith, R. L.; Rajeshwar, K. *Environ. Sci. Technol.* **1994**, *28*, 934.

(41) Bahnemann, D.; Bockelmann, D.; Goslich, R. *Sol. Energy Mater.* **1997**, *24*, 564.